EARTH SURFACE PROCESSES AND LANDFORMS
Earth Surf. Process. Landforms **44**, 2170–2185 (2019)

Published online 3 June 2019 in Wiley Online Library
(wileyonlinelibrary.com) DOI: 10.1002/esp.4640

Fluvial incision and coarse gravel redistribution across the modern Dead Sea shelf as a result of base-level fall

Haggai Eyal,[1,2] Elad Dente,[1,2] Itai Haviv,[3] Yehouda Enzel,[1] Thomas Dunne[4] and Nadav G. Lensky[2]*
[1] The Freddy & Nadin Herrmann Institute of Earth Sciences, The Hebrew University of Jerusalem, The Edmond J. Safra Campus, Givat Ram, Jerusalem 91904, Israel
[2] Geological Survey of Israel, 32 Yesha'yahu Leibowitz, Jerusalem 9371234, Israel
[3] Department of Geological and Environmental Sciences, Ben Gurion University of the Negev, Beer Sheva 84105, Israel
[4] Bren School of Environmental Science and Management, University of California-Santa Barbara, Santa Barbara, CA USA

Received 13 August 2018; Revised 29 March 2019; Accepted 15 April 2019

*Correspondence to: Nadav G. Lensky, Geological Survey of Israel, 32 Yesha'yahu Leibowitz, Jerusalem 9371234, Israel. E-mail: nadavl@gsi.gov.il

ESPL
Earth Surface Processes and Landforms

ABSTRACT: Global eustatic lowstands can expose vast areas of continental shelves, and occasionally the shelf edge and the continental slope. The degree of fluvial connectivity to receding shores influences the redistribution of sediments across these emerging landscapes. Shelf and slope emergence in the Dead Sea since the middle of the 20th century, offers a rare opportunity to examine evolution of stream connectivity in response to continuous base-level decline. We characterize the connectivity evolution of two streams, using high-resolution time series of aerial imagery and elevation models, field mapping, and grain-size analyses. Our rich spatiotemporal dataset of evolving channel geomorphology, sediment transport conditions, and sediment redistribution, allows calculating potential coarse sediment mobility in response to base level decline. Following shelf emergence, alluvial fans first prograded onto the low-gradient shelf under unfavourable conditions for transporting coarse sediment to the regressing shoreline. Then, with shelf and slope emergence, the two adjacent streams evolved differently. The smaller, more arid watershed still maintains its highstand delta progradation on the shelf and is practically disconnected from the receding lake. The larger catchment, heading in wetter environments and having a narrower shelf, has incised the shelf and renewed and gradually intensified the sediment transport from the highstand to the lowstand delta. Sediment mobilization to lowstand shorelines is controlled by the evolution of the channel profile and by the average speed of gravel transport (10s-100s m yr^{-1}). These findings from the Dead Sea are relevant to fluvial processes operating on continental shelves during glacial maxima. Streams would have commonly stored high proportions of their coarse sediment on the continental shelves rather than efficiently connecting with the lowstand level. Additionally, differences in sediment routing patterns should exist among nearby streams, primarily due to continental margin geometry and watershed hydrology. © 2019 John Wiley & Sons, Ltd.

KEYWORDS: cross-shelf channel; sediment redistribution; coarse sediment bypass; channel incision; continental shelf emergence

Introduction

Global sea-level lowstands coincide with glacial maxima (e.g., Lambeck *et al.*, 2002a), resulting in the exposure of flat continental shelves and, in some locations, of the shelf edge and parts of the continental slope (Törnqvist *et al.*, 2006). Under such conditions, a submerged landscape is exposed to subaerial geomorphic processes. Fluvial systems extend, and in places incise the shelf and adjust to the lowering and regressing coastline (Figure 1).

The fluvial system responds to regression of a water body in a variety of ways. Fluvial channels can incise significantly and form cross-shelf valleys linking highstand shorelines and the shelf edge (Blum *et al.*, 2013; Blum and Price, 1998). Then, "sediment bypass" can occur as coarse sediments traverse the shelf into the offshore basin. Such a response requires a sufficiently steep gradient to exist or to evolve across the shelf, and usually involves exposure of the shelf edge (Törnqvist *et al.*, 2006; Woolfe *et al.*, 1998). Alternatively, channels may maintain limited or no connection to the shore with only minor incision into their highstand coastal prism, forming coastal plain valleys and depositing sediment on the shelf (Blum *et al.*, 2013; Blum and Törnqvist, 2000; van Heijst and Postmal, 2001; Koss *et al.*, 1994; Nijhuis *et al.*, 2015; Törnqvist *et al.*, 2006; Woolfe *et al.*, 1998). This response takes place if the stream inflow cannot provide sufficient competence and capacity to transport the imposed sediment load across the shelf. The differing responses alter sediment coastal zone flux and storage across continental margins worldwide (Blum *et al.*, 2013; Blum and Törnqvist, 2000; Woolfe *et al.*, 1998). This range of potential responses motivates studying the underlying processes controlling the fluvial response type, and the way these processes affect the degree of connectivity of the fluvial system to the regressing shoreline and the resulting

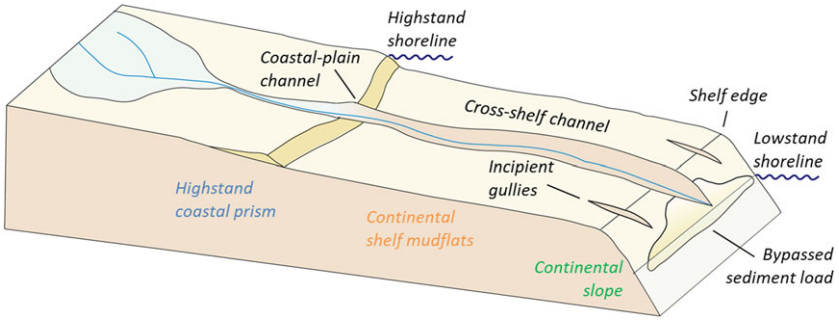

Figure 1. Schematic diagram for defining the concepts and environments in this study. [Colour figure can be viewed at wileyonlinelibrary.com]

sedimentation. Such investigations are hindered at most continental margins by postglacial inundation.

Studies of paleo-valleys, especially of late Quaternary systems (e.g. Anderson *et al.*, 2004; Druckman *et al.*, 1995; Lericolais *et al.*, 2001; Miall, 2002; Posamentier, 2001; Wellner and Bartek, 2003), have provided insights into the range of responses in various regions, especially focused on the resulting sedimentation. Because most of the shelves are now submerged, seismic and borehole data (Posamentier, 2001; Woolfe *et al.*, 1998), and bathymetry (Posamentier, 2001) are used to reconstruct the sequence of sediment redistribution. To examine specific sediment transport processes and resultant stratigraphy during sea-level fall, laboratory experiments are also used (van Heijst and Postma, 2001; Koss *et al.*, 1994; Martin *et al.*, 2009; Strong and Paola, 2006, 2010). Although very informative, the spatiotemporal scales of such experiments are limited to several meters and days, which are several orders of magnitude smaller than the natural scale of continental margin exposures of kilometres to hundreds of kilometres and millennia, respectively. Scaling up experimental results to elucidate landscape change is a challenge (Koss *et al.*, 1994). Field-scale insights are also deduced from responses to changes in the levels of lakes and reservoirs (Blum *et al.*, 2013). In such studies the documentation and analysis of channel evolution and the controls on it, can improve models of future profile and morphology evolution (e.g. Begin *et al.*, 1981; Ben-Moshe *et al.*, 2008; Dente *et al.*, 2017, 2018; Hassan and Klein, 2002). Dente *et al.*, (2017), for example, used a rare field setting and analysed the geomorphic evolution of a ~30-km-long, cross-shelf, perennial stream during the migration of a knickpoint. They showed that the main controls on the channel evolution are the initial exposed gradient at the channel mouth and the gradients of receiving and emerging bathymetry (i.e., the changing shape of the accommodation space).

In a strategy similar to flume experiments, we present a modern, field-scale analogue of a continental shelf setting that explores two contrasting responses of fluvial systems to the Dead Sea level decline. The spatiotemporal scales of these field analogues are intermediate between experiments and continental margin settings (SI 1); the evolving Dead Sea field settings are rare in the world and present fluvial evolution across several kilometres during decades. We utilize the relatively large field scales and rapid response of streams to lake level fall, to investigate the processes controlling fluvial system connectivity, coupled with coarse sediment redistribution across the shelf to the deep basin, during base level decline. In doing so, we also propose a methodology for evaluating the evolution of sediment transport and storage along streams responding to base level change. This evaluation combines spatiotemporal modelling of the channel profile, the channel cross section, and the Shields stress mobility potential. As part of the results, we present a geomorphological characterization of the studied streams, and then the evolution of the channel geomorphology and sediment transport potential. In the discussion, we focus on the controls on the degree of stream connectivity and redistribution of sediments. Finally, we generalize the insights from the sequence of processes operating at the margins of the Dead Sea to the geomorphic responses of fluvial streams to sea-level fall along continental margins worldwide.

Regional setting

Dead Sea level decline, shelf emergence, and fluvial response

The Dead Sea (Figure 2a) is a terminal lake, confined between tectonic escarpments (Figure 2b, c) and filled with late Miocene to Holocene sediments (Garfunkel and Ben-Avraham, 1996). Water diversions within the lake catchment since the mid-20th century caused a lake level fall of ~1 m yr^{-1} (Figure 2d) (Lensky *et al.*, 2005). The new, continuously emerging landscape consists of three geomorphic domains that extend eastwards from the western escarpment (Figures 1 and 2c) and are analogous to continental margin settings: (1) An alluvial sandy-gravelly highstand coastal prism with a slope of ~2%, dominated by clasts of limestone, dolomite and some chert, reworked from the upstream Cretaceous rocks and terraces. (2) A shelf, characterised by low gradient mudflats (0.5-1%), comprised of Pleistocene to Holocene, sub-horizontal, lacustrine silt, clay and aragonite laminae. (3) A steep slope (7-11%) below the shelf edge comprised of the same lacustrine sediments as the shelf. These three domains emerged sequentially over the past ~70 years (Figure 2d) at a rate two orders of magnitude larger than eustatic-level change rates (e.g. Lambeck *et al.*, 2002b).

In places, the rapid lake recession resulted in rapid incision of its tributaries (Ben-Moshe *et al.*, 2008; Bowman *et al.*, 2010; Dente *et al.*, 2017; Hassan and Klein, 2002; Vachtman and Laronne, 2006). Ben-Moshe *et al.* (2008) demonstrated that to predict longitudinal profiles of tributaries in response to the lake level fall, the time-averaged geomorphic effect of episodic flash floods and sediment transport could be represented by a continuous diffusion-type model (Begin *et al.*, 1981). Since the work of Ben-Moshe (2005), the lake level has dropped by additional ~15 m and a new landscape has been exposed, subjecting the lake margins to fluvial processes: deeper incision, knickpoint retreat and, in formerly unaffected streams, initial delivery of coarse gravel from the highstand coastal prisms to the lake.

Nahal Qumeran and Nahal Og streams

In this study we focus on Nahal Og and Nahal Qumeran, adjacent streams, flowing onto the emerging shelf at the northwestern edge of the Dead Sea (Figure 2b). Nahal Og incises

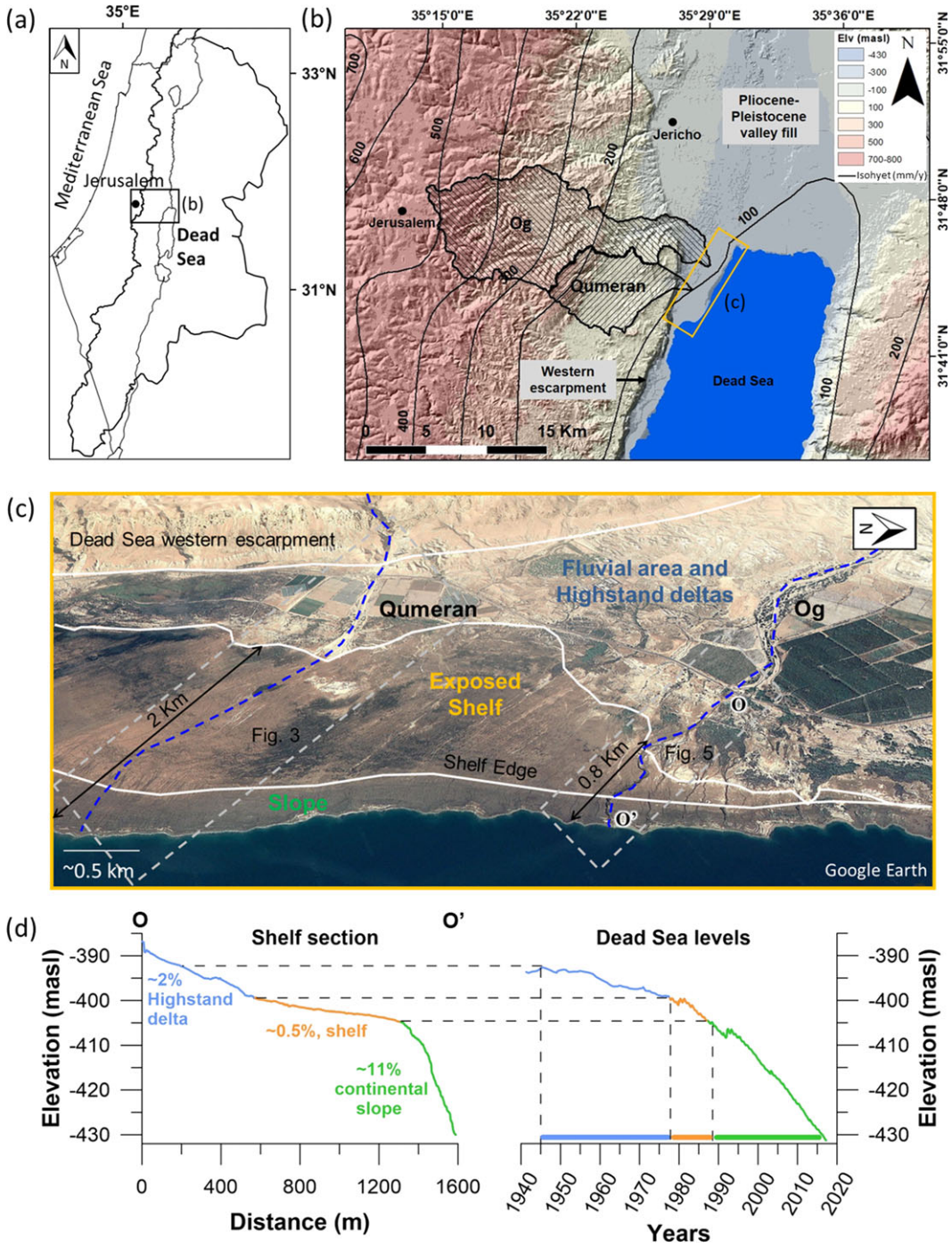

Figure 2. (a) Location map. The Dead Sea watershed is indicated by the bold black line (b) A map of the drainage basins of Nahal Og and Nahal Qumeran with isohyets (in black). The orange rectangle marks the research area extent. (c) An oblique view from east to west, toward the research area of the Og and Qumeran streams (Google Earth satellite image). (d) On left is O-O' topographic cross-section (see Figure 2c for location), which is a typical cross section of the shelf along the bank of Nahal Og. On the right, the modern Dead Sea lake level curve that drives the sequential exposure of the respective geomorphic domains. [Colour figure can be viewed at wileyonlinelibrary.com]

the shelf and transports coarse sediments across the above-mentioned three geomorphic domains, whereas Nahal Qumeran does not incise the shelf but feeds an alluvial fan that extends onto the mudflat platform. The research area is hyper-arid and subjected to infrequent rainstorms and flash floods (Cohen and Laronne, 2005; Dayan and Morin, 2006; Greenbaum *et al.*, 2006). In the headwaters of Nahal Og and Nahal Qumeran the mean annual precipitation is $>500\,mm\,yr^{-1}$ and $>200\,mm\,yr^{-1}$, respectively, whereas near the Dead Sea shore precipitation is $\sim50\,mm\,yr^{-1}$ (Figure 2b). Since no direct discharge measurements have been made in these catchments, we compare the hydrologic activity of the streams by means of the rain index (RI), which is the mean annual volume of rain falling over each basin (Ben-Moshe *et al.*, 2008; Haviv, 2007). Nahal Qumeran drainage area is $47\,km^2$ and its rainfall index is $\sim8\times10^6\,m^3\,yr^{-1}$ whereas Nahal Og has a drainage area of $137\,km^2$ and a rain index of $\sim40\times10^6\,m^3\,yr^{-1}$ (Table I). These drainage areas are far larger than those in experiments, but still smaller than watersheds of rivers along continental shelves. As reflected by its higher rain index, Nahal Og has a greater hydro-geomorphic capacity for incision and sediment transport. Peak discharges have been estimated by indirect methods after rare floods, yielding an exceptional peak discharge of 330 $m^3\,sec^{-1}$ (equivalent to an instantaneous intensity of $8.7\,mm\,hr^{-1}$ over the entire watershed) in 2006 in the Og and 150 $m^3\,sec^{-1}$ ($11.5\,mm\,hr^{-1}$) in

Table I. Hydroclimate and geomorphic characteristics of Nahal Qumeran and Nahal Og

Channel name	Drainage area (km^2)	Channel gradient* (%)	Rain index ($10^6 m^3 y^{-1}$)	Shelf width (km)	Shelf edge elevation (masl)	Shelf edge first exposure (year)
Og	127	1.15	~40	~0.8	-405	1987
Qumeran	47	1.6	~8	~2	-410	1996

*in the segment incising the old highstand deltas and not affected by lake level fall.

2007 in the Qumeran (Arbel *et al.*, 2009). In front of Nahal Qumeran, the shelf width is ~2 km and the top of the shelf edge was exposed in 1996 at a lake level of -410 masl. In front of Nahal Og, the shelf width is ~0.8 km and the top of the shelf edge was exposed in 1987 at a lake level of -405 masl. We suggest that the geomorphic setting of these two channels provides a more realistic, multi-faceted, natural analogue to global base level fall than laboratory experiments.

Data and Methods

Airborne LiDAR DEMs of the study area with a spatial resolution of 0.5 m $pixel^{-1}$ and vertical resolution of 0.25 m were acquired during April–May in the years 2011, 2013, 2014, 2015 and 2016 (Geological Survey of Israel database). Since the channels were dry during the LiDAR scans and because vegetation is scarce in the study area, these DEMs reflect the terrain and provide accurate slopes, channel longitudinal profiles, and channel cross sections. Topographic cross sections of the Og channel, measured in 2004 by Ben-Moshe (2005) with a differential GPS were also used. To examine the evolution of the longitudinal profile of the Og channel over time, profiles were projected onto a line that follows the current channel using ArcMap; this projection allows quantitative characterization and spatial comparison of the longitudinal profiles and their temporal variations (Ben-Moshe *et al.*, 2008; Davis *et al.*, 2009; Dente *et al.*, 2017). Based on the measured downstream lake level, upstream unaffected channel, and the application of a diffusion-like transport-model (Begin *et al.*, 1981), we reconstructed channel profiles at various times prior to 2004.

Orthophoto imagery and georeferenced aerial photographs with a spatial resolution of 12.5 cm and up to several meters per pixel from the years 1987, 1996, 1998, 1999, 2002, 2004, 2008, 2010, 2011, 2012, and 2015 were obtained from the Geological Survey of Israel database and from Ben-Moshe (2005). A satellite image of the study area from 1971, with a spatial resolution of ~2 m $pixel^{-1}$ was obtained from the Corona mission (Grosse *et al.*, 2005; data available from https://earthexplorer.usgs.gov). These images were used to examine landscape change preceding the available LiDAR-based DEMs. They were also used for mapping and determining the altitude of the shorelines of the 20^{th} and 21^{st} centuries, the changing spatial extent of the three geomorphic domains, channel widths and the progradation of the highstand alluvial fan of Nahal Qumeran.

The Dead Sea lake levels are available at annual resolution for the last 100 years (e.g., summary in Bookman *et al.*, 2006), and monthly resolution is available since 1976 from the Hydrological Survey of Israel. Thus, we can use the elevation of the seasonally to annually forming coastal cliffs, shorelines, and beach landforms as accurate time lines marked directly on the landscape (Ben-Moshe *et al.*, 2008).

The dark colour of the fine-grained lacustrine sediments of the shelf and its contrast with the white-grey colour of the coarser gravel, which originates in the highstand deltas and is transported across the shelf, allows easy distinction between them in the field and in orthophotographs/aerial photographs. This field contrast also facilitates clear identification of sediments that have bypassed the shelf. Thus, distinct patches of gravel that once extended along the shores can be mapped and associated with the distinct shoreline of a specific year. This enables dating of the onset of coarse sediment bypass, mapping of the distribution of bypassed material and documentation of its size distribution, and the estimation of the volume of coarse sediments transported across the shelf with an annual resolution.

With the purpose to evaluate the mobility of the coarse sediment in Nahal Og, we measured the largest 10 clasts (a, b and c axes) at: (1) Five abandoned, annually deposited, lowstand fans, preserved adjacent to the recent channel bank, (2) the 2016 active fan, and (3) the vicinity of in-channel sites of the 2016 and 2004 knickpoints. These measurements enable us to define the average maximum clast size (D_{max}) of the bypassed gravel for specific years and to estimate the bypass efficiency over time. Median particle size (D_{50}) was also determined near the 2004 and 2016 knickpoints.

Spatiotemporal evaluation of sediment transport

We propose a methodology for spatiotemporal evaluation of the dynamics of coarse sediment transport in fluvial systems responding to sea level change. The mobility of various clast sizes is defined here by Shields stress values that exceed a critical value. In order to illustrate how the mobility evolved we calculate these values along the channel longitudinal profile (x) and with time (t). The Shields stress (Buffington and Montgomery, 1998; Shields, 1936) is defined as:

$$\tau^*(S,H,D_i) = \frac{\rho g H S}{(\rho_s - \rho) g D} = 0.625 * \frac{H * S}{D_i}, \quad (1)$$

where τ^* is the Shields stress, S is the channel bed gradient, H is water depth and D_i is a specific clast size. The channel bed gradient, S (at specific x and t), is estimated from the reconstructed, evolving longitudinal channel profiles and is interpolated spatiotemporally. D_{max} gravel-sizes used in the mobility calculations were measured in the abandoned lowstand fans. Typical floodwater depths were calculated based on discharge mass conservation equation and the empirical Manning's formula:

$$Q = A * V = H * W * V \quad (2)$$

$$V = \frac{S^{\frac{1}{2}} * H^{\frac{2}{3}}}{n} \quad (3)$$

where Q is the typical annual peak discharge, V is the flow velocity, W is the channel width and n is the Manning roughness value, chosen as 0.04, which is a representative value for the channelized turbulent flow over gravely domains (Chow, 1959). The channel width, W (at specific x and t), is measured from aerial photographs, orthophotographs and surveyed

channel cross sections and is interpolated spatiotemporally. Water depths in the channel are obtained by substituting Equation (2) into (3) and inverting (3):

$$H(Q,S,W,n) = \left(\frac{Q*n}{W*S^{\frac{1}{2}}}\right)^{\frac{3}{5}} \quad (4)$$

Accordingly, the water depth, H (at specific x and t), also varies spatiotemporally.

The mean annual flood discharge was estimated from direct observations of high-water marks documented in a specific location along the channel. These flow marks were interpreted to represent a common flood peak from which a flood peak discharge of 20 m^3 sec^{-1} was calculated by Equations (2) and (3). The obtained discharge was applied to all other cross sections along the channel under the assumption that the steep confined channel and its silty bed would not allow any reduction of the peak discharge along the channel (SI 2). This discharge is chosen as representing the medium-frequency annual flood peak that carries most of the load in river channels (Wolman and Miller, 1960), although we are aware that in streams with arid to subhumid catchments the modal transporting flows are somewhat rarer than in humid regions.

The spatiotemporal Shields stress distribution for the representative discharge, τ^* (at specific x and t), is obtained by combining the spatiotemporal matrices of channel bed gradient, water depths and the specific clast size according to Equation (1). To identify the conditions for mobility we compare each value of τ^* with the critical Shields stress for transport (τ_c^*). We used two previously proposed models for estimating τ_c^*: (a) Mobility depends on interactions between each size class and the mean particle size (Ashworth and Ferguson, 1989; Komar, 1987), a measured value of D_{50} = 0.05 m was used as a representative value for the gravely domains. (b) Mobility is slope-dependent (Lamb *et al*., 2008) (SI 2). These models were developed in gravel-bed channels, whereas in the research area, the gravel on the channel bed is patchy and parts of the bed are muddy. The proposed methodology provides an ability to evaluate the dynamics of coarse sediment transport in time and space in an evolving fluvial system responding to a changing base-level.

Results

Geomorphic response of Nahal Qumeran

Nahal Qumeran does not respond to the dramatic lake level decline; its fluvial activity is limited to the highstand delta and the channel remains disconnected from the receding lake (Figure 3). This disconnectivity occurs despite: (1) the exposure of a steep near-shore slope (7%, Figure 3c), (2) a 22 m vertical difference between the shelf edge and the 2016 shore (Figure 3d), and (3) the fact that >20 years have passed since the initial exposure of the shelf edge (Figure 2d). Analysis of the channel longitudinal profile and cross sections indicates (Figure 3d, A-D): (A) minor incision in the upper part of the highstand coastal prism (which has a ~2% gradient), forming a channel with a gradient of ~1.6%. (B) Deposition of coarse gravel at the highstand prism front, localizing the apex of the current alluvial fan (Figure 4). (C) No channelization or sediment transport activity across the mudflats. (D) Formation of local gullies, each with a small drainage basin, incising the shelf edge. Since the sandy-gravelly deposits are cohesionless and are unable to sustain a bank to confine the flow, a wide, shallow, braided channel is formed migrating laterally to create an alluvial fan (Figure 4). During flash floods, downstream of the alluvial fan front water continues to flow in a very shallow braided channel on the low-gradient mudflats.

Geomorphic response of Nahal Og

Nahal Og currently crosses and incises the mudflats and slope, keeping pace with the receding lake and transports coarse gravel across the shelf to the lake shore (Figure 5). Upstream, the channel is incised into its highstand coastal prism (Figures 6a and 7a); the knickpoint is currently located near the contact between the coarse gravel and the shelf lacustrine deposits (Figures 6b and 7a). Throughout this paper, the term knickpoint refers to the most upstream abrupt change in channel gradient, although it is actually the upper part of a knickzone that extends all the way to the stream mouth as the lake continues falling (Figure 7a). Downstream, the channel deepens, forming a >10-m deep canyon, incised into the laminated lacustrine deposits of the shelf (Figure 6c), and is characterized by steep banks and a cohesive un-armoured bed with patches of gravel (Figure 6d). The deepest incision appears at the shelf edge, where bank cliffs are >20 m high. Downstream of the shelf edge, the channel is incised into the slope (Figure 6e) reaching the lakeshore and forming an active lowstand alluvial fan (Figure 6f). Gravels are currently transported from the highstand delta along the entire channel to the channel mouth. These sediments spread in annual bands along progressively lower shorelines by wave action as the stream mouth closely follows the declining level of the lake (Figure 6f). The coarse gravel deposition shows distinct northward elongation from the channel mouth forming successively longer beach ridges (Figure 5d). Upslope from the active channel mouth the coarse gravel deposits decrease in areal extent (Figure 5d). The highest appearance of a coarse gravel alluvial beach ridge is located at elevation of -415 masl (Figure 7a).

Channel evolution of Nahal Og

In the early 1970s, Nahal Og was characterized by a several hundred meters wide braided mouth, accumulating coarse sediments at the highstand delta. i.e, it was then very similar to the current morphology of the mouth of Nahal Qumeran. In the late 1970s the highstand delta was fully exposed (Figure 2d) and flash floods could spread laterally on top of the non-channelized highstand delta prism. Following the continuous recession of the lakeshore, the front of the highstand delta began to prograde slowly and to build an alluvial fan over the muddy shelf. The channel incised slightly into the highstand delta with its ~2% gradient, forming a channel with a gradient of ~1.15% (Figure 7a). Meanwhile, there was no incision across the shelf and the shelf gradient of 0.5-1% extended to the channel mouth (Figures 8a and 8b). At this stage, coarse sediments were not transportable across the shelf to the receding shoreline.

After 1987, the shelf edge was exposed and subsequently the slope with its ~11% gradient has emerged above water (Figure 2d). At this point, local gullies, each with tiny drainage basins, incised the shelf edge by knickpoint retreat (Figure 5d, SI 3). The cross-shelf channel profile steepened rapidly after the shelf slope was exposed (Figure 7a); by 1996, a shallow channel developed and connected the stream to the receding shoreline. In 1998, an avulsion of the lower ~450 m channel segment to an adjacent gully approximately 200 m to the south-west was documented; since then the channel has not shifted laterally and has incised continuously.

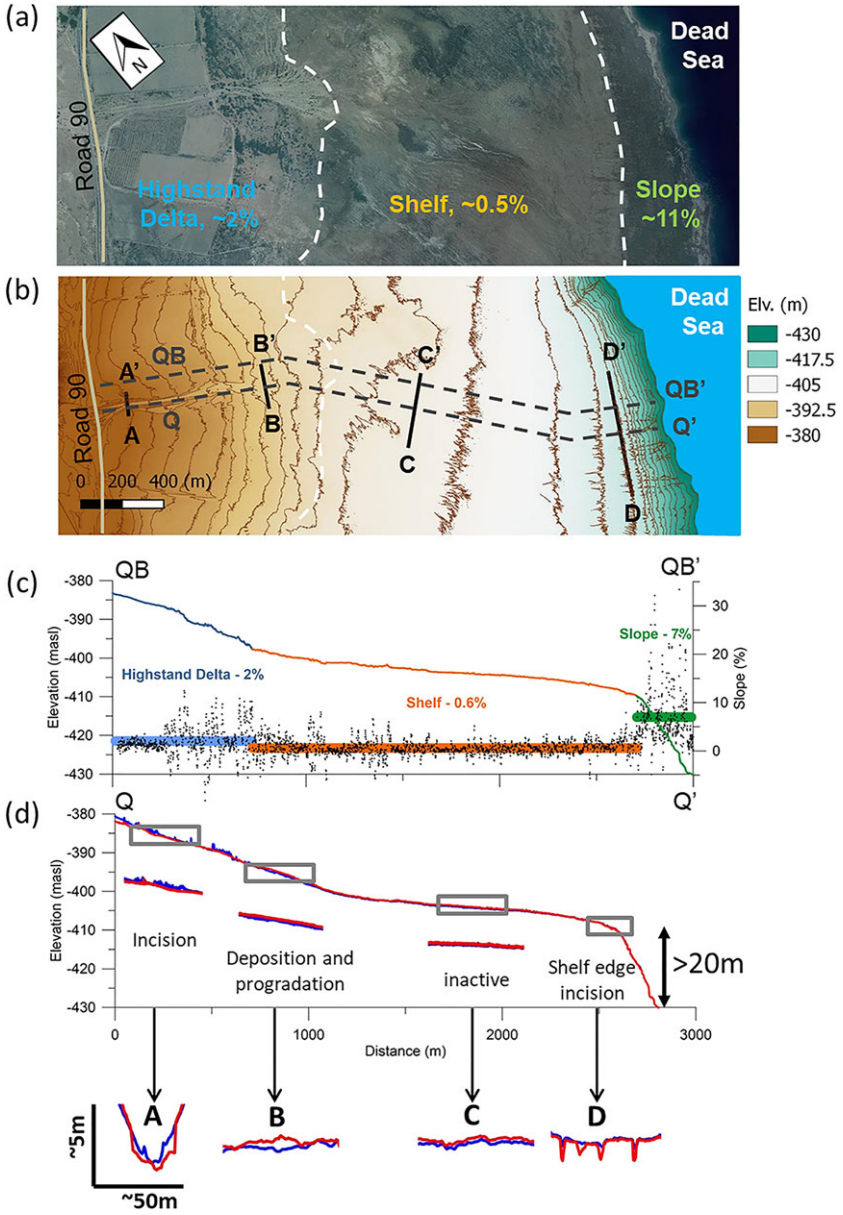

Figure 3. (a) Aerial photograph of Nahal Qumeran and its geomorphic domains (location in Figure 2c). (b) DEM with hillshade and 2-m contours. Locations of transverse (solid lines) and longitudinal (dashed lines) profiles are also marked (location in Figure 2c). (c) Typical longitudinal profile along the bank of the three geomorphic domains (solid line) and local gradients (dashed line with coloured bars indicating the average). (d) The longitudinal profiles of the Qumeran channel in 2011 (red) and 2016 (blue). The grey rectangles on the bank profile mark the locations of the enlarged segments and one cross section for each rectangle is shown below to highlight the changed fluvial morphology along the profile (see Figure 3b). [Colour figure can be viewed at wileyonlinelibrary.com]

The 2004 channel profile (Figure 7a) indicates that a knickpoint had retreated ~500 m upstream by 2004, generating a much steeper profile than the original shelf topography. Since then, the knickpoint also has begun to expand into a knickzone, leaving behind a steepened slope (Figures 7a and 8b). The channel continued to incise annually during floods, widening its banks, deepening its bed and forming an almost straight, V-shaped steep canyon (Figures 7a and 7b).

We identify two phases of upstream knickpoint-knickzone migration during the course of continuous lake-level decline. Starting from the exposure of the shelf edge in 1987, the first phase was characterized by fast knickpoint migration of 30-50 m yr^{-1} while the channel incised through the soft silt-clay lacustrine deposits before reaching the resistant coarse gravel of the highstand delta by ~2011. The second phase involved slower knickpoint migration of ~13 m yr^{-1} through the resistant coarse gravel of the highstand delta. As the knickpoint retreated headward, and especially as it approached the front of the highstand alluvial fan, it became a broader and shallower knickzone (SI 4).

Evolving sediment transport in Nahal Og

Coarse sediment transport in Nahal Og evolved with the continuous incision of the channel in response to the lake level decline. In this section, we use the Shields parameter as the index of the evolving transport potential. Figure 9 (a, b, c) shows the gradients, widths, and depths of flows in each reach and year of the channel profile's evolution. Figures 9 (d, e, f) indicate the years and reaches in which the Shields stress from Equation (1) exceeded the critical Shields stress value required for transport of fine (0.01 m), medium (0.1 m), and coarse (0.4 m) gravel respectively according to the various models for τ_c, elaborated in Section 4 and SI 2. The results in the figure are interpreted as follows.

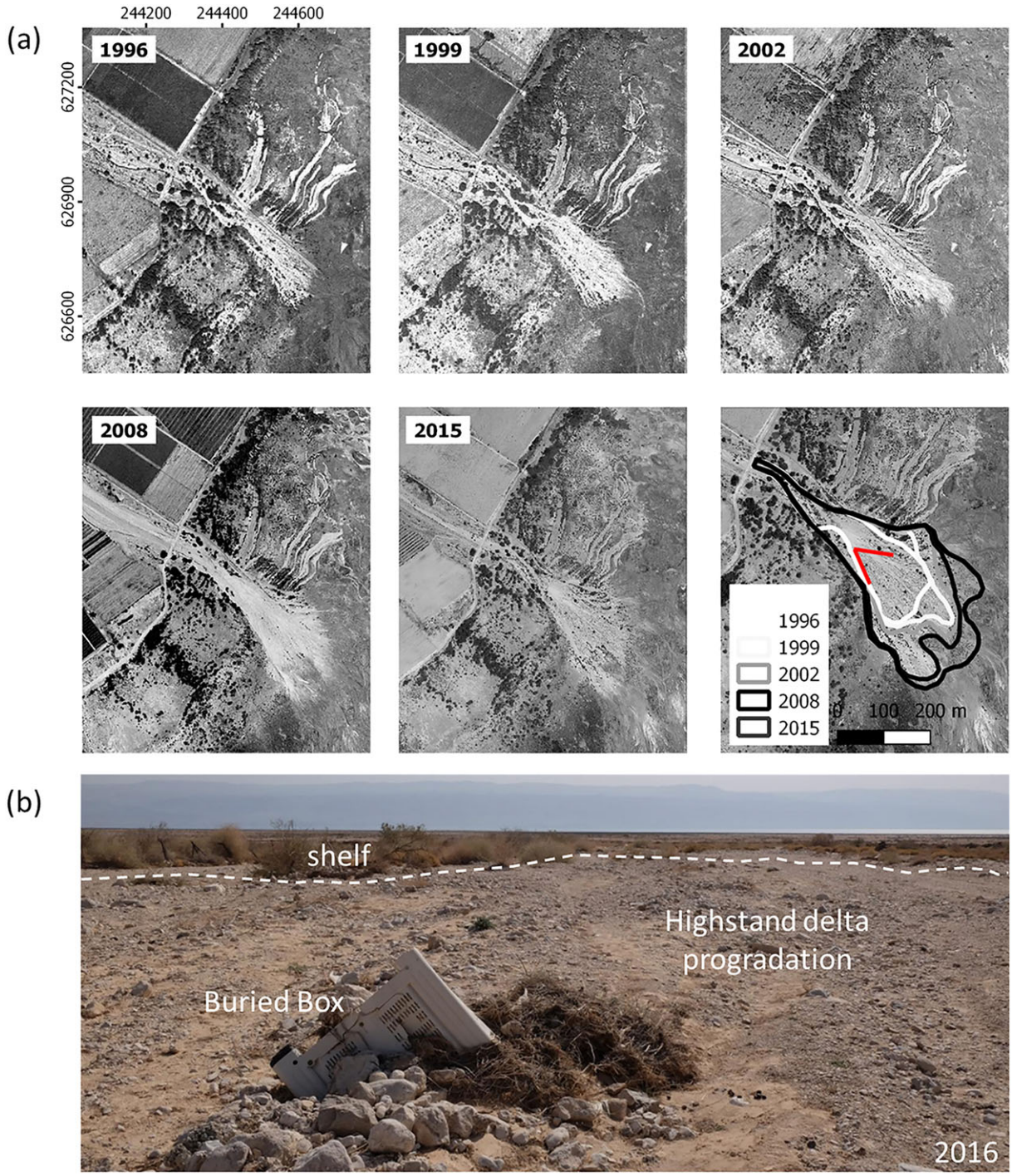

Figure 4. (a) Qumeran highstand delta progrades onto the exposed shelf. Progradation is mapped in the bottom right image of the panel. The red V-shape mark shows the orientation of the photograph that appears in Figure 4b. (b) A plastic box (~1 m long) is buried by coarse sediment of the highstand delta (view to the east, downstream). [Colour figure can be viewed at wileyonlinelibrary.com]

Following the exposure of the highstand gravel delta in the 1970s, relatively finer gravel sizes were selectively transported from the highstand delta. Thus, a lower-gradient (Figure 9a), more channelized (Figure 9b-c), channel segment was formed where the finer fraction accumulated on the shelf at the delta front. The Shields calculation predicts that transport of fine and medium clasts (i.e. D_i=0.01 m and D_i=0.1 m, respectively) and channel incision across the highstand delta have occurred since the 1970s (Figure 9d, e). The Lamb *et al*. (2008) model always predicted transport across the entire domain for the finer fraction (SI 2). Channelization and coarsening of the highstand delta continued following the exposure of the low gradient shelf (late 1970s to late 1980s), leading to limited progradation of cohesionless sand and gravel finer than 0.1 m, across the fan-shelf boundary (Figures 7a and 5a). The slight gravel progradation did not significantly alter the original shelf gradient.

After 1987, following the exposure of the shelf edge and the steep shelf slope, a knickpoint began migrating upstream, evolving with time into a broader knickzone. The knickzone migration accelerated channel incision (Figure 7a); the channel bed steepened (Figure 9a), narrowed (Figure 9b) and flow depth during floods increased accordingly (Figure 9c). Therefore, after 1987, the Shields stress increased through time at each point along the channel and progressively coarser clast fractions became mobile (Figures 8c, 9e and 9f). The predicted conditions for transport of medium size gravels (~0.1 m) across the highstand delta were established in the late 1970s to mid-1990s and across the entire shelf during the mid to

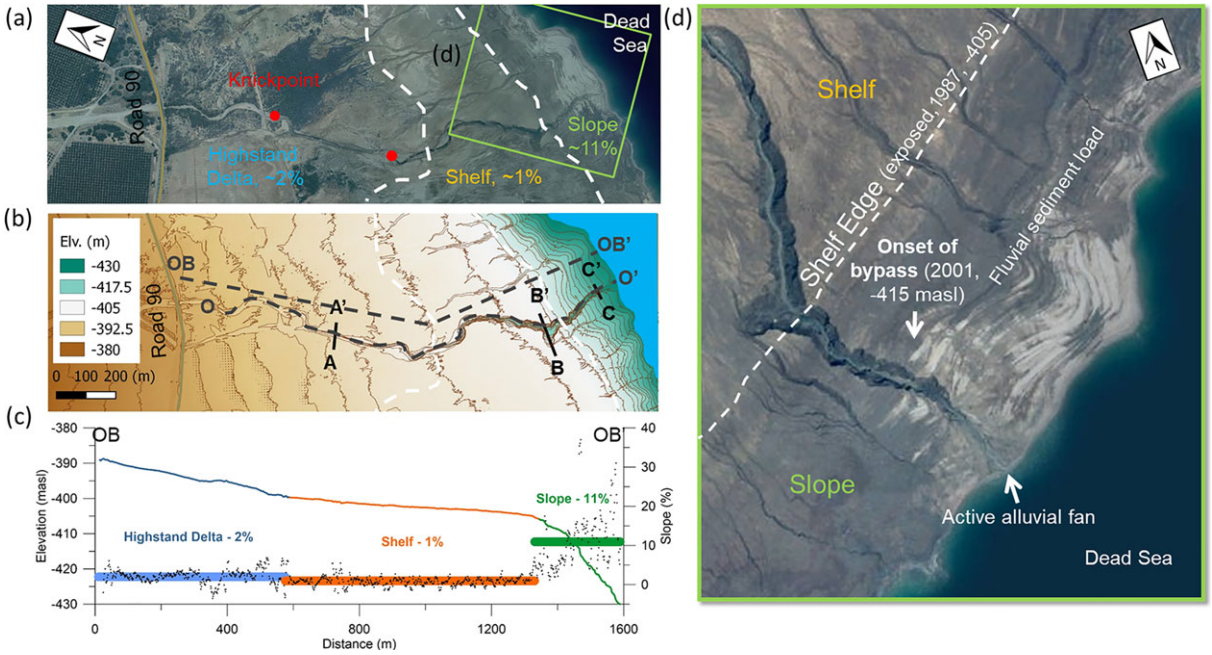

Figure 5. Geomorphic characterization of Nahal Og. (a) Aerial photograph (location in Figure 2c). Geomorphic domains are indicated with their slopes and divided by dashed white lines; knickpoint locations are indicated by red dots (upstream - 2016, downstream - 2004). The green box is expanded in d. (b) Hillshaded DEM with 2 m contours, showing locations of cross sections (solid black lines) and channel (O-O′) and bank (OB-OB′) profiles (dashed black lines), presented in Figures 5c and 7. (c) Typical bank longitudinal profile, showing the three geomorphic domains (solid line) and local gradients (black dots and coloured bars indicating the average slope). (d) Aerial photograph of Nahal Og mouth and shelf edge. Bypassed gravels with white appearance, detected in the aerial photograph, are deposited mostly north of the channel mouth in the form of beach ridges. [Colour figure can be viewed at wileyonlinelibrary.com]

Figure 6. Photographs from Nahal Og arranged from its upstream knickpoint down to the coastline (arrows pointing downstream). (a) Knickpoint area, characterized by the transition from the highstand gravely bed to the shelf muds. (b) Outcrop at the knickpoint, showing coarse gravel of the highstand delta overlying lacustrine deposits. (c) Cross-shelf channel. (d) The muddy channel bed with a sparse cover and patches of individual gravel clasts. (e) The channel incising the shelf edge and slope, viewed from the shelf edge. (f) The channel mouth. (g) The uppermost (i.e. the first arrival) coarse gravel deposit overlying the muddy slope; this observation represents the onset of accelerated cross-shelf coarse gravel transport in 2004. (h) Bank outcrop near the lakeshore showing the bypassed gravelly sediments overlying lacustrine deposits. (i) Alongshore northward transport of the coarse gravel in 2016). [Colour figure can be viewed at wileyonlinelibrary.com]

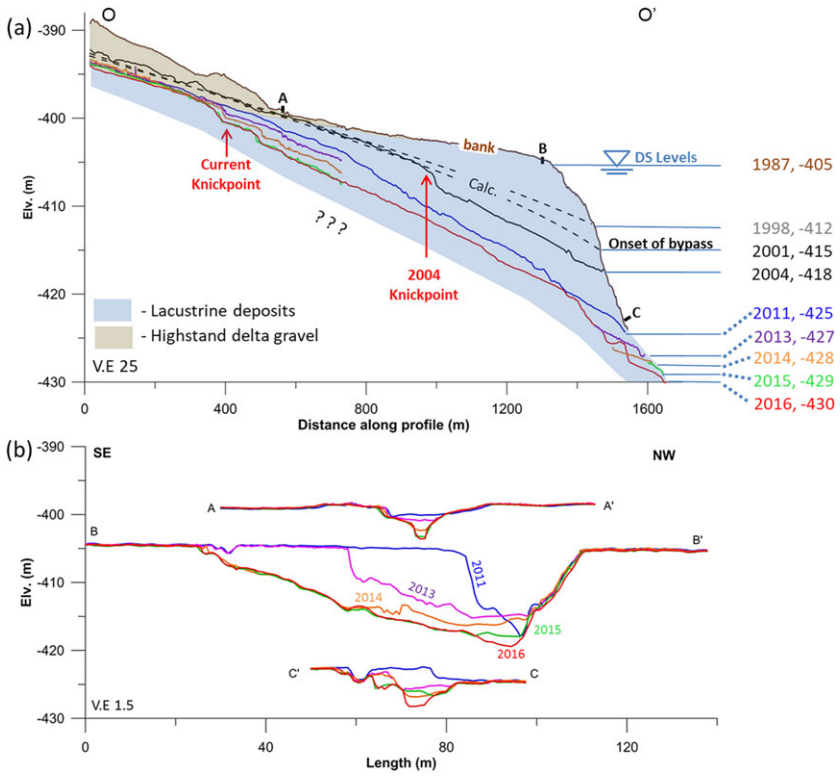

Figure 7. (a) Longitudinal profile evolution of Nahal Og (location in Figure 5b). Bank profile represents the initial pre- 1987 geometry. The calculated profiles of 1998 and 2001 (labelled "Calc."), are based on the measured downstream lake level and upstream unaffected channel, and the reconstructed profile by a diffusion-like transport-model (Begin *et al.,* 1981; Ben Moshe *et al.,* 2008). The channel deepens and lengthens annually, and the profile evolves as an expanding knickzone characterized by sharp step at its upstream end, i.e. the knickpoint. (b) Cross sections showing channel deepening over time. [Colour figure can be viewed at wileyonlinelibrary.com]

late-1990s (Figure 9e). However, medium size gravels (D_{max}<0.11±0.03 m) were first observed arriving at the lowstand fan in 2001. These sediments defined the onset of bypass and formed the first lowstand alluvial fan, with its gravel that in part transformed into a beach ridge by waves (Figures 5d, 6g and 7a).

With continuing lake level decline, the upstream migrating knickzone expanded into the zone of coarse gravel, establishing the conditions for the mobility of even the coarser gravel across the shelf. The intensification of the bypass of the coarse sediments is documented by the increase in both gravel size and volume reaching the lowstand fan (Figures 8c-d, 6g-6i, and SI 5 and 6).

The conditions for transport of the coarsest gravel fraction available in the upstream knickpoint source region (D_{max}<0.41±0.11 m) were established in the more evolved bypass stage, i.e. since 2000-2010 (Figure 9f). However, only in 2016, did we observe this gravel size (D_{max}<0.42±0.09 m) arriving at the lowstand fan. The observations (Figure 8c) and the Shields stress calculations (Figure 9f) show that since 2016 all clast sizes in Nahal Og should be mobile across the shelf to the lowstand lake shoreline. The Lamb *et al.* (2008) model never predicted transport across the shelf for the coarse fraction (SI 2).

Discussion

Contrasting connectivity of adjacent fluvial systems in the Dead Sea

Qumeran and Og are adjacent channels, characterized by highstand coarse-clastic deltas, and both drain to wide, low-gradient mudflats and steep, shelf-margin slopes, subjected to the same lake level fall. However, the response of these two channels to the lake level drop is fundamentally different. Nahal Qumeran is characterized by continuous on-shelf highstand delta progradation without any incision into the shelf. Nahal Og incises the slope, shelf, and highstand delta and transports coarse sediment across the shelf through its deep, incised channel to form a lowstand coarse-clastic delta at the shoreline.

The smaller drainage basin of Qumeran is entirely arid to hyperarid in comparison with the larger and wetter catchment of Nahal Og, which receives more frequent eastern Mediterranean rainstorms (Dayan and Morin, 2006); the Nahal Og rain index is 6-7 times larger (~8×10^6 m^3 yr^{-1} and ~50×10^6 m^3 yr^{-1}, respectively). The rain index determines whether the potential energy gradient that is stored in the shelf edge, can be exploited to initiate shelf incision and form a new channel. The wider shelf (>2 km) in front of Nahal Qumeran in contrast with the 0.8-km wide shelf in front of the Og, further reduces the potential to incise a channel connected with the lowering shore. Hence, the wider shelf and the more arid, smaller basin combine to reduce the ability of Nahal Qumeran to incise the shelf and connect with the shore. The influence of drainage area and the geometry of the lake margins on the fluvial connectivity is further discussed in SI 7. Consequently, the coarse-gravel deposits of the highstand delta remain impeded by low gradients, are incapable of reaching much beyond the delta edge, and continue to contribute to the ongoing progradation of the on-shelf alluvial fan (Figure 4). At the shelf edge, incision is restricted to the tiny local drainages forming small gullies of limited length and minimal knickpoint retreat (Figure 3d) (Koss *et al.*, 1994; Woolfe *et al.*, 1998). Based on our field experience in that area and our analysis, we hypothesize that under an extreme future storm and flood Nahal

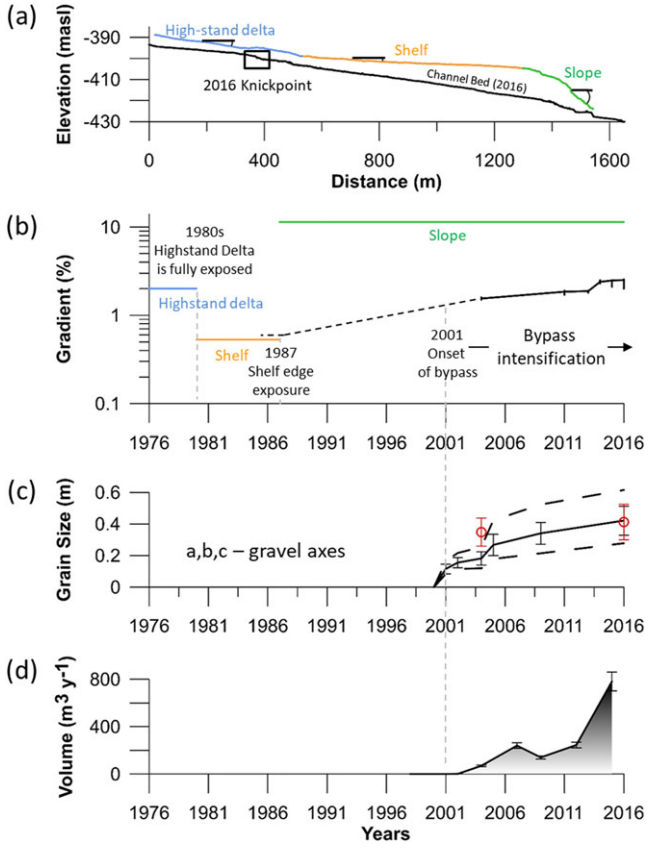

Figure 8. Onset and intensification of coarse gravel bypass. (a) Longitudinal profile (2016) of channel bed and bank, colour coding (from Figure 5c) indicates the three geomorphic domains; the 2016 knickpoint is indicated. (b) The evolution of the knickpoint gradients during the successive exposure of the three domains with gradient indicated by the same colour coding as in Figure 5c; solid line – measured data, dashed line - interpolation. (c) The evolution of gravel size measured in abandoned annual lowstand deposits. Solid line - average D_{max} of gravel b-axis values, dashed lines - average D_{max} of gravels a- and c- axes values. Red circles indicate average D_{max} of gravel b-axis in the upstream knickpoints of 2004 and 2016 (SI 5). The increase in D_{max} over time is statistically significant (SI 5). (d) The evolution of bypassed sediment volumetric flux deposited as beach ridges in the lowstand delta (SI 6). [Colour figure can be viewed at wileyonlinelibrary.com]

Qumeran could initiate incision of the shelf. At this point it is difficult to propose the needed magnitude-duration of such an event. The Nahal Qumeran record, thus, demonstrates that the interval of highstand delta deposition and progradation can extend into lowstand intervals, producing out-of-phase fluvial response among basins with different drainage areas, hydroclimatology, and shelf geometries.

In Nahal Og, the narrower shelf and wetter basin-wide hydroclimatology promote faster responses to the same magnitude of lake level fall and incision across the entire shelf. The evolution of a channel profile into an extensive upstream migrating knickzone with a gradually steepening channel upstream (Figure 7a and Figure S11b) was reported based on laboratory experiments of knickpoint evolution in non-cohesive material (Brush and Wolman, 1960). However, the Bush and Wolman (1960) experiment, as well as many others that followed, used a single base-level fall at the inception of the experiment that produced gradient reduction and channel widening downstream of the knickzone. In Nahal Og, the upstream migration of the knickzone forced the steepening and narrowing in the downstream reach because of the continuing decline of the base level as the Begin *et al.* (1981) and Ben Moshe *et al.* (2008), profile evolution models would have predicted. The response of the channel profile to continuous base level decline should better represent the conditions during global sea-level fall, even though the rate of base level decline in the Dead Sea is larger than in the global sea level fall.

Coarse sediment transport in fluvial systems responding to base level fall

Here the discussion focuses on the evolution of coarse sediment mobility in Nahal Og, in response to base level fall and presents the processes controlling mobility and redistribution of coarse sediments. This is based on the insights gained from the Shields stress analysis and from the field observations. The highstand deltas in both Nahal Qumeran and Nahal Og evolve with the declining level of the lake and the emergence of the low-gradient shelf (late 1970s to 1987). The coarse sediments encountered the shelf where they were deposited as a prograding ramp. These coarse sediment ramps are cohesionless and unable to confine the flow to a single channel and the flow spreads widely as a braided fan (Murray and Paola, 1994). The observed progradation across the fan-shelf boundary is not predicted by the Shields stress calculation (Figures 9d-9f) without higher, less frequent flow discharges (SI 2). Wolman and Miller (1960) support this assertion and suggest that when the variability of the flow increases (i.e. in small and arid catchments) a larger percentage of the total load is carried by less frequent flows. The time interval during which the highstand deltas can potentially prograde across the shelf is bounded by the timing of the shelf edge exposure. This interval is controlled directly by the rate of base level decline and local shape of the shelf and slope. A shoreline retreat rate that exceeds the rate of highstand delta progradation, can result in a highstand delta, which is limited to the top of the shelf, as in the deltas of Nahal Og and Nahal Qumeran. However, horizontal retreat rate of the shoreline equal or lower than the rate of highstand delta progradation, can result in deltas keeping pace with the regressing shoreline and depositing coarse sediments across the entire shelf, as in the lowstand deltas of the large rivers draining into the Gulf of Mexico (e.g. Anderson *et al.*, 2016).

After 1987, Nahal Og stopped prograding its alluvial fan and its fluvial transport and deposition shifted to a lowstand phase. Following the exposure of the shelf edge and its high-gradient slope, the potential of Nahal Og to incise the cohesive muds comprising the shelf gradually formed a confined channel through which a knickzone retreated upstream from the declining base level. Confinement of the flow and the evolving gradient increased the transport competence of the channel. Thus, channelized gravel transport could begin with the onset of upstream knickzone migration, even prior to arrival of the distinct knickpoint at the gravel source region in the highstand delta. Since the mid-1990s, most gravel-size classes can be transported across the shelf (Figure 9). Indeed, quite coarse clasts (D_{max}<0.35±0.09 m) were measured on an abandoned terrace of the 2001-2004 incised channel at the mid-shelf location, prior to the knickpoint arrival upstream to the high-stand delta. The 1998 channel avulsion probably slowed the transport along the lower segment of the channel as a less steep and wider gully was occupied by this avulsion. As the knickpoint reached the clast source region (at the 2001-2004 knickpoint location, Figure 7a), the mobility and transport rates of all gravel-size classes increased along the entire channel, reaching the regressing shoreline (Figures 8 and 9). The increase in transport capacity of the channel is attributed mainly to the continuously exposed steep gradients at the channel

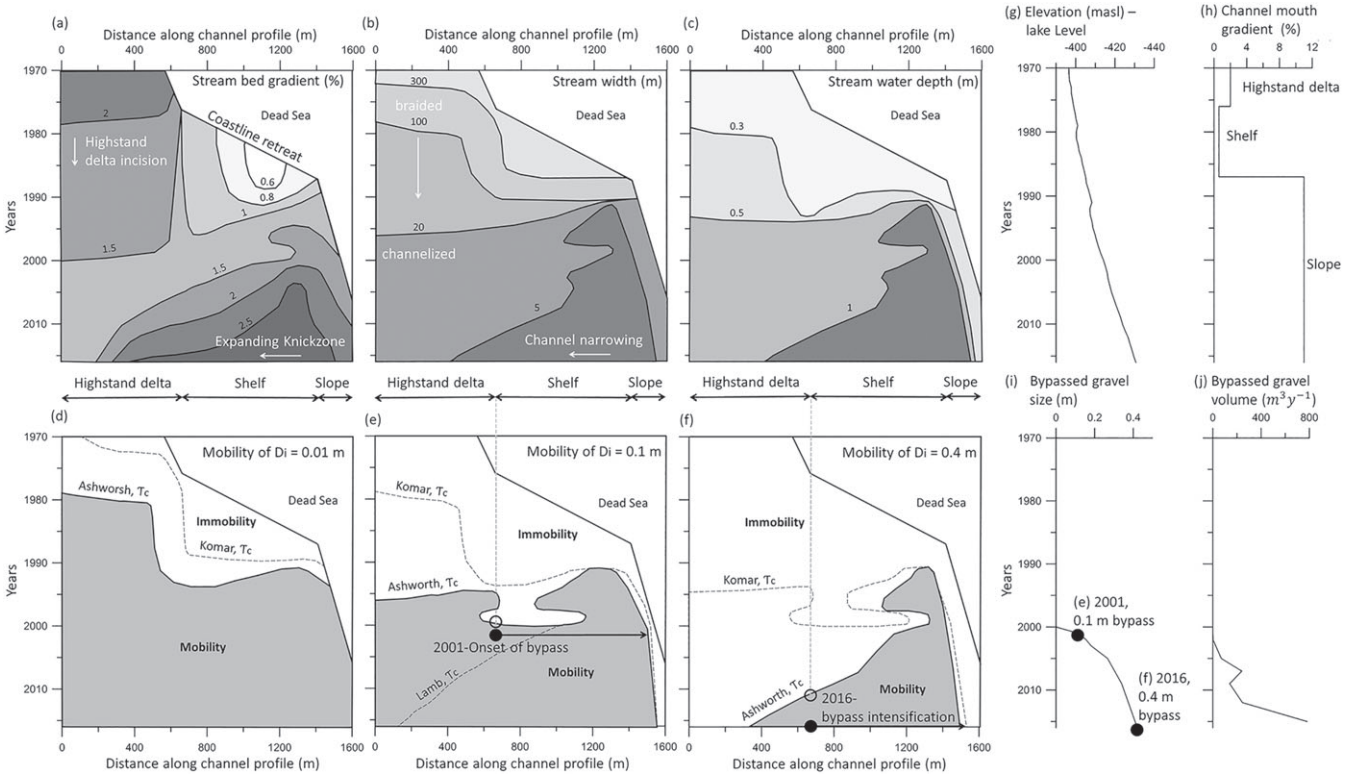

Figure 9. Spatiotemporal mobility of coarse sediments along Nahal Og. The analysis follows the methodology presented in Section 4. The horizontal axis is the distance along Nahal Og longitudinal profile (e.g. Figure 7a) and the vertical axis is the time. (a) Stream bed gradients, (b) stream width, (c) computed water depths during a typical flood of 20 m^3 sec^{-1} (SI 2). The calculated "mobility" and "immobility" fields are marked in Figures 9d-f for fine to coarse gravel size classes. In (g) and (h) temporal variations of the lake level and the sequential exposed mouth gradients are presented, respectively. (i) Bypassed gravel size (D_{max}) measured in the lowstand abandoned fans, with time. Black dots denote the D_{max}=0.1 m measured at the onset of bypass in 2001, and the D_{max}=0.4 m, representing the largest gravels available for transport from the highstand to the lowstand delta at 2016. The gravels from these two transport events (black dots) were sheared from the highstand delta; we present the source of these gravels in the spatiotemporal diagrams (e) and (f) as solid black dots. The predicted mobility in 2004 and 2016 are presented as open circles in (e) and (f), accordingly. Note that observed values are delayed in time by a few years. (j) Volumetric flux of the bypassed gravel. The predictions by Komar's (1987), and by Ashworth and Ferguson's (1989) models seem to better predict the observed transport situation in Nahal Og (SI 2).

mouth (Dente *et al.*, 2017). The accelerating rate of lake level fall (Figure 9g) amplifies this increase but a constant or slower rate of base level decline should generally produce a similar geomorphic response.

A lag-time in the transport of the coarse sediments to the lowstand shoreline exists between the predicted timing of each gravel-size class becoming mobile and its actual observed arrival to the lowstand fan (Figures 9e and 9f), although the predicted onset of mobility is obviously affected by our choice of a representative discharge. It seems that the lag-time is controlled by the time interval required to generate the necessary number of short-duration floods for sustaining gravel transport across the shelf. The average travel distance of gravel particles per event, i.e. the gravel virtual velocity (Hubbell and Sayre, 1964), is likely to be only tens of meters, as measured in gravel-bed streams (Reid and Dunne, 1996). In fact, a similar virtual velocity was measured at an upstream channel segment of Nahal Og (Hassan *et al.*, 1991). The virtual velocity is roughly adequate to explain the transport lag-time, as is demonstrated by the intensified transportation. Fine-medium gravel (D_{max}<0.1 m) prograded ~400 m on the 0.5-0.1% shelf gradient over ~10-15 years (late-1970s to early-1990s), at a virtual rate of 20-40 m yr^{-1}. Medium gravel (D_{max}<0.1 m) travelled ~500 m in the channel over 2-6 years (mid-1990s to late-1990s-2001), at a virtual rate of 80-250 m yr^{-1}. Coarse gravel (D_{max}<0.4 m) travelled ~1 km in the channel over 6-16 years (2000/2010-2016, Figures 7a and 8c), at a virtual rate of 60-160 m yr^{-1}. The increase in virtual velocity, from tens of meters to hundreds of meters, is probably related to the steepening and narrowing of the channel and hence to the increased Shields stress (Figure 7a, Figure 9).

Similarly, at the global scale, large rivers with lower gradients and finer bedload transport coarse sediment in a sequence of alternating steps and rest intervals of random length and duration in bars (Hubbell and Sayre, 1964). Thus, we generalize the concept of sediment mobilization by typical virtual velocities acting as factor affecting the lag-time to other fluvial systems such as large rivers with finer bed-material loads. In the case of lowland rivers with floodplains responding to sea-level decline, the lag time would be increased further by floodplain sediment exchange. However, the relevance of the concept is reflected in even the simple case of coarse bedload transport in Nahal Og.

Geomorphic responses of fluvial systems to base-level fall

As proposed above, the fluvial changes at the Dead Sea margins are intermediate in their spatiotemporal scales between 10^4 and 10^5 years and 1-100 km at continental margins exposed during glacial intervals and experimental studies with scales of a few meters and durations of hours or days. Here, we compare the processes at the Dead Sea margins with the larger scale changes at a setting forced by eustatic global sea-level changes (for more detailed scale comparisons see SI 1). According to our results, we propose four principal types of

river response to identical sea-level fall. In the first type, *the regressing shoreline remains above the shelf edge* (Figure 10a). In the other three types, *the regressing shoreline is below the shelf edge* and the different fluvial responses can be distinguished by the discharge (i.e. drainage basin size and hydroclimate) and shelf geometry (Figure 10b-10d).

(a) In the case of *Basin A* (Figure 10a), the regressing shoreline is above the shelf edge, and *the shelf edge remains submerged*. The average depth of the shelf edge at non-glaciated margins is 130 m (Shepard, 1963) and ranges from <100 m to ≥200 m (Törnqvist *et al*., 2006). Thus, even during the most pronounced last glacial lowstand of 120-130 m below the present level (e.g. Austermann *et al*., 2013; Clark and Mix, 2002), many continental shelves could have remained disconnected from deeper marine environments (Törnqvist *et al*., 2006). Under such conditions, fluvial activity would be confined to the shelf, forming coastal-plain valleys and prograding highstand coastal prisms of relatively coarse sediments (Figure 10a) (e.g. Posamentier, 2001; Talling, 1998). It seems that this fluvial response would have been common and cross-shelf valley formation would have been the exception, as most shorelines were situated above the shelf edge elevation throughout the LGM (and most likely during the smaller preceding glacial periods). Moreover, end-members of full glacial or interglacial sea levels are rare and brief, and a constantly changing sea-level is the rule (e.g. Lambeck *et al*., 2002a); the most persistent sea levels over the last 500 ky were around 85 m, 40 m, and 5 m below the present level (Harris *et al*., 2016). Additionally, although the shelf edge depth could have changed by tens of meters since the LGM due to sedimentation (e.g. Eckles *et al*., 2004; Simms *et al*., 2006) and isostasy (Hutton *et al*., 2013), there is a consensus that the shelf edge approximately coincides with the lowstand shoreline (Törnqvist *et al*., 2006; Vanney and Stanley, 1983). Thus, most of the time the shoreline was located above the shelf edge, even if its elevation or location changed.

(b) In *Basin B* (Figure 10b), although sea level is located below the shelf edge, no or only *limited fluvial connectivity* develops because of the combination of low stream discharges and a relatively wide shelf. Where watersheds are small, and

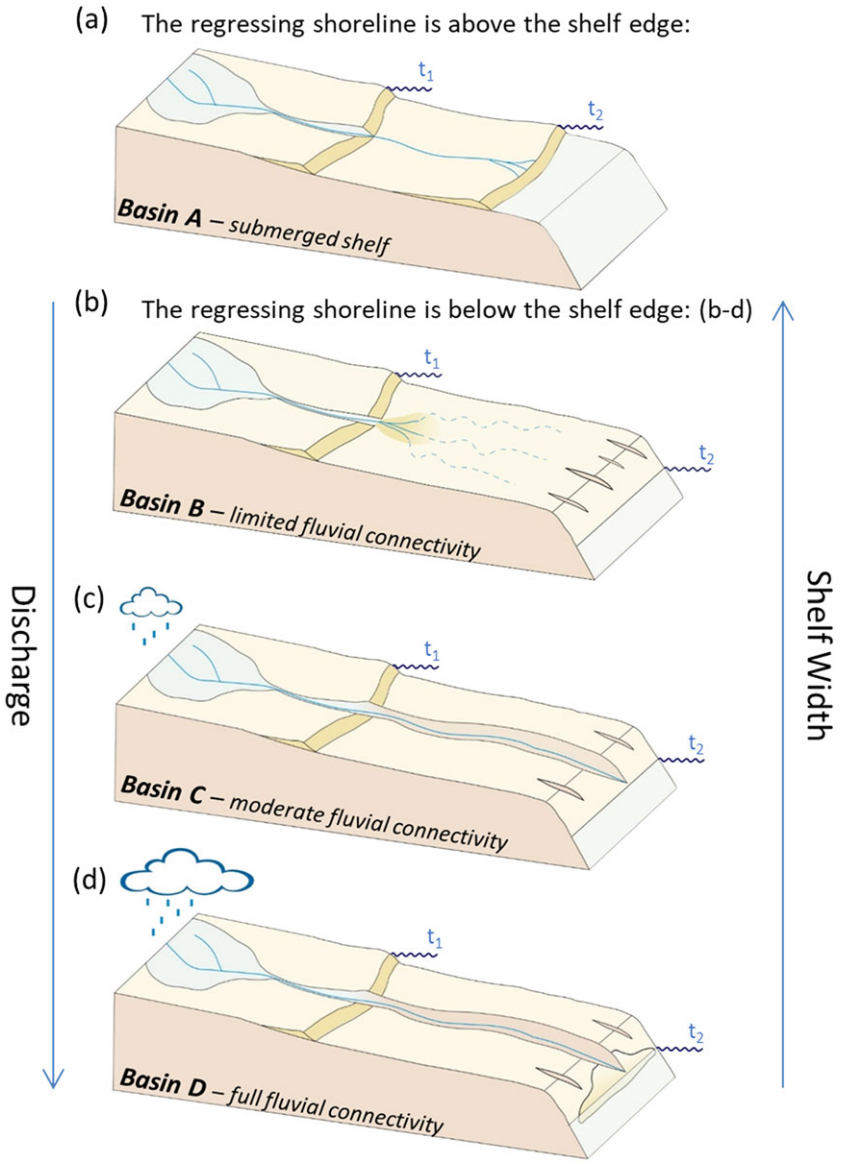

Figure 10. Schematic illustration of potential coeval responses of adjacent streams to sea level fall (Basins A-D). t1 and t2-mark highstand and lowstand phases of the base level, respectively. (a) The regressing shoreline remains above the shelf edge and a coastal plain valley is formed. (b) Formation of a coastal plain valley and incision of incipient gullies. (c) Formation of a cross-shelf valley. (d) Sediment redistribution and shelf bypassing of coarse sediment. The effect of increasing drainage basin size and hydroclimatology (represented by discharge) on the connectivity of the fluvial response is represented by the trend of the arrow pointing down from (b) to (d), and the effect of increasing shelf width on connectivity is represented in the right arrow pointing up. [Colour figure can be viewed at wileyonlinelibrary.com]

flood discharges are limited by aridity, continental and deep marine environments can remain fluvially disconnected. In such cases, fluvial activity is restricted to incision of shallow coastal-plain valleys and progradation of highstand coastal sedimentary prisms, together with minor incision of small, short channels at the shelf edge. Discharge of water and sediment decrease downstream of the hinterland, and consequently coarse sediments remain trapped on the continental shelf. The fluvial disconnection depicted in Figure 10b is amplified when the shelf is relatively wide (e.g. Nahal Qumeran). This scenario was previously referred to as an initial stage in the development of cross-shelf sedimentary environments (e.g. van Heijst and Postmal, 2001; Koss *et al.*, 1994). However, results from the Dead Sea emphasize that such conditions may persist long enough to constitute a non-transitional phase, which can be reflected in the geological record, depending on the duration of the disconnection. In the Qumeran case, the vertical difference between the shelf edge and the shoreline is ~20 m with slope gradient of 7% (2016), similar in magnitude to the vertical difference during prominent global sea-level falls; for example, in the LGM ~40 m of the shelf edge and continental slope were exposed in the Gulf of Mexico (Törnqvist *et al.*, 2006). The most extreme sea-level lowstands lasted ≤10 ky, i.e., <10% of the duration of the last glacial–interglacial cycle (Lambeck *et al.*, 2002b). Thus, in a similar manner to the current conditions in the Qumeran channel, during the relatively short interval of maximum sea-level lowstands, many rivers draining into the ocean were probably unable either to incise and bypass the shelf with coarse sediments. Such streams may have remained disconnected from the sea, leaving most of their respective coarse sediment loads upstream on the shelf. For example, the major rivers of the Great Barrier Reef, which are mostly ephemeral and have alluvial beds, did not incise the shelf during the LGM (Woolfe *et al.*, 1998). These rivers show that aggradation can occur across the entire shelf if the shelf is broad, characterized by a low gradient (0.05%-0.08%) and discharges are relatively small (Woolfe *et al.*, 1998). The disconnect between channels and the deep ocean during lowstands could be common and incised cross-shelf channels may be rare in ancient shelf successions.

(c) In *Basin C* (Figure 10c), *moderate fluvial connectivity* would evolve under higher and more frequent flows and low, finer-grained sediment loads on shelves of intermediate width. These conditions would tend to hasten the connection of the continental and deep marine segments by increasing the probability of incision of cross-shelf channels. In such cases, the coarse sediment flux may only partially reach the deep marine environment (e.g., Nahal Og pre-2001).

(d) In *Basin D* (Figure 10d), a wetter hydroclimate, larger flows and/or more frequent floods, and a narrow shelf, results in *full fluvial connectivity*. Channel incision would be faster and the flux of coarse sediment to the sea would be renewed quickly following sea-level decline and would intensify rapidly thereafter (e.g. Nahal Og post-2001). For example, during the LGM in the Gulf of Mexico, the Trinity, Sabine, Brazos, and the Colorado Rivers and the Rio Grande crossed the entire shelf, depositing lowstand deltas on the shelf margin (Anderson *et al.*, 2004, 2016; Simms *et al.*, 2006). The adjacent Nueces River and nearby small rivers flowed across a ramp-like shelf and incised valleys that extended only to the middle shelf; their inability to cross the shelf is related to either antecedent topography on the shelf (Anderson *et al.*, 2004; Simms *et al.*, 2006) or relatively small sediment supply (Anderson, 2005). This example demonstrates the potential influence of high variability in hydroclimate and shelf geometry between adjacent rivers that respond to the same eustatic decline. Full connectivity could be slowed down or accelerated by a wider or narrower shelf, respectively. As cross-shelf valley formation is related to sea levels reaching to below the shelf edge (Figures 10c-10d) and appears to be the exception, a longer extreme lowstand could enable widespread shelf incision and coastal/deltaic progradation to the shelf edge. Full fluvial connectivity can be attributed to: (1) intervals dominated by the 10^6 yr third-order cycles (Törnqvist *et al.*, 2006), which are seen as resulting from a combination of tectonic and glacio-eustatic accommodation changes (Strasser *et al.*, 2000) or (2) exceptional events such as the proposed Mediterranean Sea-level decline during the Messinian Salinity Crisis (e.g. Clauzon *et al.*, 1996; Madof *et al.*, 2019).

Conclusions

This study documents and explores a real-time, natural, field-scale analogue of streams responding to sea-level fall. Our observations from the emerging shelf of the Dead Sea are intermediate in scale between laboratory experiments and continental shelf and slope settings. This allows direct observations of sediment dispersal from source to sink during sea-level lowering. Following the emergence of shelf and slope, the morphological evolution and sediment redistribution of two adjacent contrasting streams were studied. A rich dataset of the morphological evolution is presented spatiotemporally, i.e. varying annually along the channel, by the measured channel bed elevation and the channel width; water depth is calculated based on channel geometry and discharge. The sediment transport evolution is then represented by the calculated Shields stress mobility potential that varies along the 1970s to 2016 channel profiles.

Nahal Og has incised rapidly and coarse sediment transport across the shelf has been established a decade and a half after the emergence of the steep shelf slope. Since then the bypassed gravel size and sediment flux have intensified. The evolution of coarse sediment transport is controlled by the channel profile, which steepens and deepens through the upstream migration of an expanding knickzone. The calculated Shields mobility calculation expresses the implications of this profile evolution for coarse sediment transport. Furthermore, it assists in explaining the observed delay in the arrival of coarse sediments to the lowstand shoreline after they were mobilized from the highstand delta. This delay is the result of the low frequency of floods and the limited transport distance of the gravels during individual short-duration (hours), flash floods.

A different response is observed in the fluvially disconnected Qumeran channel, where the highstand alluvial fan progrades on the shelf but there is no development of a channel capable of transporting coarse sediment across the shelf to the receding lake. This is despite the emerging of a >20 m vertical difference between the highstand fan and the shelf edge. The field evidence indicates that such disconnection can persist rather than being a transitional phase to a through-flowing stream (as in the case of Nahal Og).

The sedimentary record of sea-level retreat and the storage of coarse sediment on continental shelves therefore, will depend on the duration of the disconnection, which we have related to catchment scale and hydroclimatology and to shelf geometry. The global variation of these geographical attributes indicates that continental margins should be characterized by spatial and temporal variations of sediment routing patterns even between nearby rivers, such as occurs among rivers flowing across the Gulf of Mexico shelf (e.g. Anderson, 2005).

Acknowledgements—We thank the devoted team from Geological Survey of Israel and the Hebrew University – Ziv Mor, Ido Sirota, Itzik Hamdani, Ali Arnon, Amir Megides, Amir Shvit, Hallel Lutzky, Raanan Bodzin, Uri Malik, Oria Vaanunu and Bat Sheva Cohen. We appreciate

contributions from and discussions with Efrat Morin, Moshe Armon, Lior Enmar, Amir Eyal and Elisa Kagan. We also acknowledge Rivka Amit for her insights. The research was funded by the Israeli Government under GSI DS project 40572, by the Israel Science Foundation grants: 1471/18 to NL and 946/18 to YE. HE was supported by the Pfeifer Fellowship. Interested readers can access our data by contacting haggai.eyal@mail.huji.ac.il.

References

Anderson JB. 2005. Diachronous development of late Quaternary shelf-margin deltas in the northwestern Gulf of Mexico: implications for sequence stratigraphy and deep-water reservoir occurrence. SEPM Special Publication No.83.

Anderson JB, Rodriguez A, Abdulah KC, Fillon RH, Banfield LA, McKeown HA, Wellner JS. 2004. Late Quaternary stratigraphic evolution of the Northern Gulf of Mexico Margin. SEPM Special Publication No.79: 1–23.

Anderson JB, Wallace DJ, Simms AR, Rodriguez A, Weight RWR, Taha ZP. 2016. Recycling sediments between source and sink during a eustatic cycle: Systems of late Quaternary northwestern Gulf of Mexico Basin. *Earth-Science Reviews* **153**: 111–138.

Arbel S, Getker M, Arazi A, Yosi B, Moshe G, Efraim F, Alon M. 2009. Data of rain and floods of exceptional events in the hydrological year 2006-2007, special report M-84.

Ashworth PJ, Ferguson I. 1989. Size-Selective Load Entrainment of Bed in Gravel Bed Streams. *Water Resources Research* **25**: 627–634. https://doi.org/10.1029/WR025i004p00627.

Austermann J, Mitrovica JX, Latychev K, Milne GA. 2013. Barbados-based estimate of ice volume at Last Glacial Maximum affected by subducted plate. *Nature Geoscience* **6**: 553–557. https://doi.org/10.1038/ngeo1859 [online] Available from: http://dx.doi.org/10.1038/ngeo1859.

Begin ZB, Meyer DF, Schumm SA. 1981. Development of longitudinal profiles of alluvial channels in response to base-level lowering. *Earth Surface Processes and Landforms* **6**: 49–68. https://doi.org/10.1002/esp.3290060106.

Ben-Moshe L. 2005. longitudinal profiles of alluvial streams in response to Twentieth century changes in Dead Sea level, Hebrew University of Jerusalem.

Ben-Moshe L, Haviv I, Enzel Y, Zilberman E, Matmon A. 2008. Incision of alluvial channels in response to a continuous base level fall: field characterization, modeling, and validation along the Dead Sea. *Geomorphology* **93**: 524–536.

Blum MD, Price DM. 1998. Quaternary alluvial plain construction in response to glacio-eustatic and climatic controls, Texas Gulf Coastal Plain. *Relative Role of Eustasy, Climate, and Tectonism in Continental Rocks* **59**: 31–48. [online] Available from:. http://sp.sepmonline.org/content/sepsprre/1/SEC3.abstract.

Blum MD, Törnqvist TE. 2000. Fluvial responses to climate and sea-level change: A review and look forward. *Sedimentology* **47**: 2–48. DOI: https://doi.org/10.1046/j.1365-3091.2000.00008.x [online] Available from: http://doi.wiley.com/10.1046/j.1365-3091.2000.00008.x%5Cnpapers3://publication/doi/10.1046/j.1365-3091.2000.00008.x

Blum MD, Martin J, Milliken K, Garvin M. 2013. Paleovalley systems: Insights from Quaternary analogs and experiments. *Earth-Science Reviews* **116**: 128–169. https://doi.org/10.1016/j.earscirev.2012.09.003 [online] Available from: http://dx.doi.org/10.1016/j.earscirev.2012.09.003.

Bookman R, Bartov Y, Enzel Y, Stein M. 2006. Quaternary lake levels in the Dead Sea basin: two centuries of research. *Geological Society of America Spacial Paper* **401**: 155–170. https://doi.org/10.1130/2006.2401(10). For [online] Available from, http://books.google.com/books?hl=en&lr=&id=hU73uKLdYwkC&oi=fnd&pg=PA155&dq=Quaternary+lake+levels+in+the+Dead+Sea+basin+:+Two+centuries+of+research&ots=u74MEfKWHH&sig=6CxX-Nn-Sk0nwQkaA_GE22mEy9s.

Bowman D, Svoray T, Devora S, Shapira I, Laronne JB. 2010. Geomorphology Extreme rates of channel incision and shape evolution in response to a continuous, rapid base-level fall, the Dead Sea, Israel. *Geomorphology* **114**: 227–237. https://doi.org/10.1016/j.geomorph.2009.07.004 [online] Available from:, https://doi.org/10.1016/j.geomorph.2009.07.004.

Brush JLM, Wolman GM. 1960. Knickpoint behavior in noncohesive material: A laboratory study. *Geological Society of America Bulletin* **71**: 59–74.

Buffington JM, Montgomery DR. 1998. A systematic analysis of eight decades of incipient motion studies, with special reference to gravel-bedded rivers. *Water Resources Research* **33**: 1993–2029. https://doi.org/10.1029/97WR03138.

Chow V. 1959. *Open-channel hydraulics*: McGraw-Hill New York.

Clark PU, Mix AC. 2002. Ice sheets and sea level of the Last Glacial Maximum. *Quaternary Science Reviews* **21**: 1–7.

Clauzon G, Suc JP, Gautier F, Berger A, Loutre MF. 1996. Alternate interpretation of the Messinian salinity crisis: Controversy resolved? *Geology* **24**: 363–366. https://doi.org/10.1130/0091-7613(1996)024<0363:AIOTMS>2.3.CO;2.

Cohen H, Laronne JB. 2005. High rates of sediment transport by flashfloods in the Southern Judean Desert, Israel. *Hydrological Processes* **19**: 1687–1702. https://doi.org/10.1002/hyp.5630.

Davis M, Matmon A, Zilberman E, Porat N, Gluck D, Enzel Y. 2009. Bathymetry of Lake Lisan controls late Pleistocene and Holocene stream incision in response to base level fall. *Geomorphology* **106**: 352–362. https://doi.org/10.1016/j.geomorph.2008.11.014 [online] Available from: http://dx.doi.org/10.1016/j.geomorph.2008.11.014.

Dayan U, Morin E. 2006. Flash flood – producing rainstorms over the Dead Sea: A review. *Geological Society of America* **401**: 53–62. https://doi.org/10.1130/2006.2401(04). [online] Available from:, http://books.google.com/books?hl=en&lr=&id=hU73uKLdYwkC&oi=fnd&pg=PA53&dq=Flash+flood+?+producing+rainstorms+over+the+Dead+Sea:+A+review&ots=u77FEaEZHI&sig=y1kW3rIe-rGOJLY9UdmxOOpk1_k.

Dente E, Lensky NG, Morin E, Grodek T, Sheffer NA, Enzel Y. 2017. Geomorphic Response of a Low-Gradient Channel to Modern, Progressive Base-Level Lowering: Nahal HaArava, the Dead Sea. *Journal of Geophysical Research: Earth Surface* **122**: 2468–2487.

Dente E, Lensky NG, Morin E, Dunne T, Enzel Y. 2018. Sinuosity evolution along an incising channel: New insights from the Jordan River response to the Dead Sea level fall. *Earth Surface Processes and Landforms*. https://doi.org/10.1002/esp.4530.

Druckman Y, Buchbinder B, Martinotti GM, Tov RS, Aharon P. 1995. The buried Afiq Canyon (eastern Mediterranean, Israel): a case study of a Tertiary submarine canyon exposed in Late Messinian times. *Marine Geology* **123**: 167–185. https://doi.org/10.1016/0025-3227(94)00127-7.

Eckles BJ, Fassell ML, Anderson JB. 2004. Late Quaternary evolution of the wave – storm-dominated central Texas shelf. SEPM Special Publication No.79: 271–287.

Garfunkel Z, Ben-Avraham Z. 1996. The structure of the Dead Sea basin. *Tectonophysics* **266**: 155–176. https://doi.org/10.1016/S0040-1951(96)00188-6.

Greenbaum N, Ben-Zvi A, Haviv I, Enzel Y. 2006. The hydrology and paleohydrology of the Dead Sea tributaries. In *New Frontiers in Dead Sea Paleoenvironmental Research*, Enzel Y, Agnon A, and Stein M (eds). Geological Society of America; [online] Available from: https://doi.org/10.1130/2006.2401(05)

Grosse G, Schirrmeister L, Kunitsky VV, Hubberten H. 2005. The use of CORONA images in remote sensing of periglacial geomorphology: an illustration from the NE Siberian coast. *Permafrost and periglacial processes* **16**: 163–172.

Harris PT, Harris PT, Macmillan-lawler M. 2016. Seafloor Mapping along Continental Shelves. **13** DOI: https://doi.org/10.1007/978-3-319-25121-9 [online] Available from: http://link.springer.com/10.1007/978-3-319-25121-9

Hassan MA, Klein M. 2002. Fluvial adjustment of the Lower Jordan River to a drop in the Dead Sea level. *Geomorphology* **45**: 21–33. https://doi.org/10.1016/S0169-555X(01)00187-8.

Hassan MA, Church M, Schick AP. 1991. Distance of movement of coarse particles in gravel bed streams. *Water Resources Research* **27**: 503–511. https://doi.org/10.1029/90WR02762.

Haviv I. 2007. *Mechanics, morphology and evolution of vertical knickpoints (waterfalls) along the bedrock channels of the Dead Sea western tectonic escarpment*. The Hebrew University of Jerusalem.

van Heijst MWIM, Postmal G. 2001. Fluvial response to sea-level changes: A quantitative analogue, experimental approach. *Basin Research* **13**: 269–292. https://doi.org/10.1046/j.1365-2117.2001.00149.x.

Hubbell DW, Sayre WW. 1964. Sand transport studies with radioactive tracers. *Journal of the Hydraulics Division* **90**: 39–68.

Hutton EWH, Syvitski JPM, Watts AB. 2013. Isostatic flexure of a finite slope due to sea-level rise and fall. *Computers and Geosciences* **53**: 58–68. https://doi.org/10.1016/j.cageo.2012.03.020.

Komar PD. 1987. Selective grain entrainment by a current from a bed of mixed sizes: a reanalysis. *Jour. Sed. Petrology* **57**: 203–211. https://doi.org/10.1306/212F8AE4-2B24-11D7-8648000102C1865D.

Koss JE, Ethridge FG, Schumm SA. 1994. An experimental study of the effects of base-level change on fluvial, coastal plain and shelf systems. *Journal of Sedimentary Research* **B64**: 90–98. https://doi.org/10.1306/d4267f64-2b26-11d7-8648000102c1865d [online] Available from: http://jsedres.sepmonline.org/cgi/content/abstract/64/2b/90.

Lamb MP, Dietrich WE, Venditti JG. 2008. Is the critical shields stress for incipient sediment motion dependent on channel-bed slope? *Journal of Geophysical Research: Earth Surface* **113**: 1–20. https://doi.org/10.1029/2007JF000831.

Lambeck K, Esat TM, Potter EK. 2002a. Links between climate and sea levels for the past three million years. *Nature* **419**: 199–206. https://doi.org/10.1038/nature01089.

Lambeck K, Yokoyama Y, Purcell T. 2002b. Into and out of the last glacial maximum: Sea-level change during oxygen isotope stages 3 and 2. *Quaternary Science Reviews* **21**: 343–360. https://doi.org/10.1016/S0277-3791(01)00071-3.

Lensky NG, Dvorkin Y, Lyakhovsky V, Gertman I, Gavrieli I. 2005. Water, salt, and energy balances of the Dead Sea. *Water Resources Research* **41**: 1–13. https://doi.org/10.1029/2005WR004084.

Lericolais G, Berné S, Féniès H. 2001. Seaward pinching out and internal stratigraphy of the gironde incised valley on the shelf (bay of biscay). *Marine Geology* **175**: 183–197. https://doi.org/10.1016/S0025-3227(01)00134-7.

Madof AS, Bertoni C, Lofi J. 2019. Discovery of vast fluvial deposits provides evidence for drawdown during the late Miocene Messinian salinity crisis, *Geology* **47**: 171–174.

Martin J, Paola C, Abreu V, Neal J, Sheets B. 2009. Sequence stratigraphy of experimental strata under known conditions of differential subsidence and variable base level. *AAPG Bulletin* **93**: 503–533. https://doi.org/10.1306/12110808057.

Miall AD. 2002. Architecture and sequence stratigraphy of Pleistocene fluvial systems in the Malay Basin, based on seismic time-slice analysis. *AAPG bulletin* **86**.

Murray AB, Paola C. 1994. A cellular model of braided rivers. *Nature* **371**: 54.

Nijhuis AG, Edmonds DA, Caldwell RL, Cederberg JA, Slingerland RL, Best JL, Parsons DR, Robinson RAJ. 2015. Fluvio-deltaic avulsions during relative sea-level fall. *Geology* **43**: 719–722. https://doi.org/10.1130/G36788.1.

Posamentier HW. 2001. Lowstand alluvial bypass systems: incised vs. unincised. *AAPG bulletin* **85**: 1771–1793.

Reid LM, Dunne T. 1996. *Rapid evaluation of sediment budgets*: Catena Verlag Reiskirchen.

Shepard FP. 1963. Thirty-five thousand years of sea level. In *Essays in Marine Geology,* Clements T, (ed). University of Southern California Press: Los Angeles, California; 1–10.

Shields A. 1936. Application of Similarity Principles and Turbulence Research to Bed-Load Movement. *Mitt. Preuss. Versuchsanst. Wasserbau Schiffbau* **26**: 47. https://doi.org/10.1061/(ASCE)0733-9429(1995)121:11(766).

Simms AR, Anderson JB, Taha ZP, Rodriguez AB. 2006. Overfilled versus Underfilled Incised Valleys: examples from the Quaternary Gulf of Mexico. *Incised Valleys in Time and Space*: 117–139. https://doi.org/10.2110/pec.06.85.0117 [online] Available from:, http://archives.datapages.com/data/sepm_sp/SP85/Overfilled_Versus_Underfilled.pdf%0Ahttps://pubs.geoscienceworld.org/books/book/1135/chapter/10567753/.

Strasser A, Hillgärtner H, Hug W, Pittet B. 2000. Third-order depositional sequences reflecting Milankovitch cyclicity. *Terra Nova* **12**: 303–311. https://doi.org/10.1046/j.1365-3121.2000.00315.x.

Strong N, Paola C. 2006. Fluvial Landscapes and Stratigraphy in a Flume. *The Sedimentary Record* **4**: 4–9.

Strong N, Paola C. 2010. Valleys That Never Were: Time Surfaces Versus Stratigraphic Surfaces--Reply. *Journal of Sedimentary Research* **80**: 4–5. https://doi.org/10.2110/jsr.2010.007 [online] Available from: http://jsedres.sepmonline.org/cgi/doi/10.2110/jsr.2010.007.

Talling PJ. 1998. How and where do incised valleys form if sea level remains above the shelf edge? *Geology* **26**: 87–90. https://doi.org/10.1130/0091-7613(1998)026<0087:HAWDIV>2.3.CO.

Törnqvist TE, Wortman SR, Mateo ZRP, Milne GA, Swenson JB. 2006. Did the last sea level lowstand always lead to cross-shelf valley formation and source-to-sink sediment flux? *Journal of Geophysical Research: Earth Surface* **111**: 1–13. DOI: https://doi.org/10.1029/2005JF000425

Vachtman D, Laronne JB. 2006. Formation of stream channels during continuous base level lowering, exemplified at Ein-Fesh'ha, the Dead Sea, Israel. *EGU conference poster* **8**: 7962.

Vanney SJ-R, Stanley DJ. 1983. Shelf break Physiography: An Overview. *SEPM* **33**: 1–24.

Wellner RW, Bartek LR. 2003. The Effect of Sea Level, Climate, and Shelf Physiography on the Development of Incised-Valley Complexes: A Modern Example From the East China Sea. *Journal of Sedimentary Research* **73**: 926–940. https://doi.org/10.1306/041603730926 [online] Available from:, http://jsedres.sepmonline.org/content/73/6/926.abstract.

Wolman MG, Miller JP. 1960. Magnitude and Frequency of Forces in Geomorphic Processes. *The Journal of Geology* **68**: 54–74. https://doi.org/10.1086/626637 [online] Available from:, https://www.journals.uchicago.edu/doi/10.1086/626637.

Woolfe KJ, Larcombe P, Naish T, Purdon RG. 1998. Lowstand rivers need not incise the shelf: An example from the Great Barrier Reef, Australia, with implications for sequence stratigraphic models. *Geology* **26**: 75–78. https://doi.org/10.1130/0091-7613(1998)026<0075:LRNNIT>2.3.CO;2.

Supporting Information

Additional supporting information may be found online in the Supporting Information section at the end of the article.

Table S1: The parameters used in the calculations
Table S2: The mean of the largest 10 clasts and the standard deviation measured at various locations along Nahal Og.
Table S3: Bypassed sediment volume. These data appear graphically in Fig. 9d.
Figure S1: Channel bed gradients (S) Matrix.
Figure S2: Channel width (W) matrix.
Figure S3: Water depth (H) matrix.
Figure S4: Dimensionless Shields stress for the 0.01 m fraction, Critical Shields stress according to Ashworth and Ferguson (1989) and Komar (1987) are indicated on the bottom of the Diagram. D_{50} = 0.05 m was used.
Figure S5: Dimensionless Shields stress for the 0. 1 m fraction, Critical Shields stress according to Ashworth and Ferguson (1989) and Komar (1987) are indicated on the bottom of the Diagram. D_{50} = 0.05 m was used.
Figure S6: Dimensionless Shields stress for the 0.01 m fraction, Critical Shields stress according to Ashworth and Ferguson (1989) and Komar (1987) are indicated on the bottom of the Diagram. D_{50} = 0.05 m was used.
Figure S7: Mobility of the 0.01 m fraction according to Lamb (2008).
Figure S8: Mobility of the 0. 1 m fraction according to Lamb (2008).
Figure S9: Mobility of the 0.4 m fraction according to Lamb (2008).
Figure S10: Sections along the shelf edge of Nahal Og (shaded relief map presnts the section location).
Figure S11: Knickpoint-knickzone evolution in Nahal Og. (a) Knickpoint upstream migration and incision over time, (b)

Temporal changes in channel gradients showing the lengthening of the knickpoint over time, (c) incision above and below the knickpoint, incision is greater below the knickpoint (d) gradient evolution over time below and above the knickpoint, gradient increase is greater below the knickpoint.

Figure S12: Linear regression between the accumulation year of the lowstand abandoned fans and the D_{max} of the measured samples. We show here the data for the axis of the gravel, but the same results were obtained for the means of all three gravel axes.

Figure S13: ANOVA test results for gravel B axis measurement D_{max}. Years (Levels) that are not connected by the same letter are significantly different at the 0.05 level. 2004N and 2016N represent the samples measured at the knickpoint location in these two years; the rest of the years represent the samples measured in lowstand abandoned fans at Nahal Og mouth.

Figure S14: Schematic illustration of the geometry of coarse deposits along beach ridges.

Figure S15: (a) Envelope curve of channel gradient vs. drainage area for alluvial channels (Montgomery and Buffington, 1997). Og and Qumeran channels are plotted in red and blue dots, respectively (Table 1 in the manuscript). The Dead Sea shelf and slope gradients are marked using dashed horizontal lines and the global shelf and slope gradients are marked with solid black lines (references for the global gradients are included in SI 1). (b) Schematic illustration of three alluvial channels with drainage areas of A1>A2>A3, the streams are assumed to have quasi-steady channel width and identical hydroclimatology. For the largest channel the difference between channel gradient and the gradient of the shelf (ΔS1) is smallest. Channel 2 will take longer to initiate full bypass as the shelf gradient must increase by a higher value (ΔS2, dashed arrow) for full bypass to occur. Channel 3 has the smallest drainage area and its transportation gradient is higher than the continental slope gradient. Thus, the transportation gradient required for full bypass (ΔS3, dotted arrow) cannot be reached.

Data S1. Supporting Information